Title: Improving the measurement of dielectric function by TEM-EELS: avoiding the retardation effect

Authors: Norihito Sakaguchi*, Luka Tanda, Yuji Kunisada

Affiliation: Laboratory of Integrated Function Materials, Center for Advanced Research of Energy and Materials, Faculty of Engineering, Hokkaido University

Address: Kita-13, Nishi-8, Kita-ku, Sapporo, Hokkaido 060-8628, Japan

Running title: Improving dielectric function measurement

*Corresponding author
Norihito Sakaguchi
Tel & Fax: +81-11-706-6768
E-mail: sakaguchi@eng.hokudai.ac.jp
Address: Kita-13, Nishi-8, Kita-ku, Sapporo, Hokkaido 060-8628, Japan

Total page: 16
# of Figures: 9

Abstract

We investigated an improved Kramers–Kronig analysis (KKA) routine for measuring the dielectric function of α-Al_2O_3, avoiding the retardation effect arising in electron energy-loss spectroscopy (EELS). The EELS data differed from the optical data in the energy range of 10–20 eV due to the retardation effect, even though Cerenkov loss was thoroughly suppressed. The calculated differential cross-section indicates that the influence of the retardation appears at scattering angles less than 0.2 mrad in the loss energy range of 10–15 eV. Using the improved KKA routine, we obtained the correct dielectric function that agreed with the optical data. The present technique is especially useful in measuring the dielectric function by EELS with a small collection semi-angle.

Introduction

Kramers–Kronig analysis (KKA) is a useful technique for determining the optical properties of materials from electron-energy loss spectroscopy (EELS) data in the low-loss region. This technique is sometimes called valence EELS (VEELS), and by coupling VEELS with transmission electron microscopy (TEM), one can obtain optical properties with a higher spatial resolution than that possible by using usual optical techniques [1–3].

One substantial problem in using VEELS to characterize actual materials is Cerenkov losses, which occur when electrons in the medium travel faster than the speed of light. The medium can produce other low-energy losses as well, from retardation of electrons [4–7]. One simple way to avoid Cerenkov losses is to decrease the TEM accelerating voltage below a threshold known as the Cerenkov limit [8–10]. For example, 60-kV TEM can measure VEELS data without Cerenkov losses in materials with a refractive index less than 2.2; however, in this case the retardation effect of the electrons still influences the data.

In the present study, we demonstrate how the retardation effect affects the measurements of the dielectric function of α-Al_2O_3 by using

low-voltage TEM-EELS, and we propose an improved KKA procedure that removes the retardation effect from the VEEL spectra.

Methods

To prepare the TEM samples, a (0001) α-Al_2O_3 wafer with the refractive index of 1.76 (λ = 500 nm) was cut into pieces, mechanically polished down to 20 μm, and then ion-milled by PIPS (Gatan model 691). The accelerating voltage and incident angle of the Ar^+ ion were 4 kV and 5°, respectively. TEM and EELS measurements were performed using a TEM (FEI Titan^3 G2 60-300) equipped with an image filter (Gatan model 965). The accelerating voltage of the TEM was set to 60 kV or 300 kV. VEELS spectra were acquired in selected-area electron diffraction (SAED) mode with a dispersion of 0.05 eV/ch, using a SAED aperture with a diameter of 100 nm. The collection semi-angles of the EELS detector were set to 0.3 and 2 mrad.

The dielectric function was derived from the VEEL spectra based on the procedure from Egerton [11]. All of the spectra were corrected for plural scattering events by Fourier-log deconvolution. Zero-loss fitting was performed with the reflected tail method. The single scattering distribution

(SSD) was then angular corrected and normalized to obtain the energy-loss function (ELF). Finally, the real and imaginary parts of the dielectric function $\varepsilon = \varepsilon_1 + i\varepsilon_2$ were obtained by using the Kramers–Kronig relations.

Results and discussions

Figure 1 shows the real (ε_1) and imaginary (ε_2) parts of the dielectric function, ε, obtained by TEM-EELS and conventional KKA. In this figure, the dotted lines express the dielectric function derived from the optical measurement [12]. We acquired the VEEL spectra without influence from Cerenkov radiation by reducing the acceleration voltage to 60 kV. The overall shape of the dielectric functions measured at various collection semi-angles agreed with the optical data; however, obvious differences appeared in the energy range of 10–20 eV. Note that this difference was clear in the measurement at a smaller correction semi-angle. Generally, when comparing the VEELS and optical data, it is better to use a smaller collection-semi angle in the VEELS measurements because the finite size of the collection-semi angle allows for momentum transfer during the electron excitation. Thus, these results are slightly abnormal. We considered the

surface loss as one cause, but our sample was ~100 nm thick, and almost all of the influence of surface loss would be removed by using the present KKA procedure proposed by Egerton [11]. Another cause might be the retardation effect, but we used sufficiently slow electrons.

Figure 2 shows a calculated double-differential cross-section of the inelastic scattering based on Kröger's theory [13] using the dielectric function provided by the optical measurement. This figure uses a colored logarithmic scale, and plots the double-differential cross-section as a function of energy loss and scattering angle. This figure only plots the volume loss term, which is expressed as follows based on Erni's formula [6]:

$$\frac{\partial\sigma_i}{\partial\Omega\partial E} \propto \mathrm{Im}\left[\frac{1}{\hat{\varepsilon}}\frac{1-\hat{\varepsilon}(v_e/c)^2}{\theta^2+{\theta_E}^2\{1-\hat{\varepsilon}(v_e/c)^2\}}\right], \quad (1)$$

where σ_i is the cross-section of the inelastic scattering, Ω is the solid angle, E is the energy loss, $\hat{\varepsilon}$ is the complex conjugate of the dielectric function, v_e is the electron velocity, c is the speed of light in vacuum, θ is the scattering angle, and θ_E is the characteristic angle of the inelastic scattering. When the retardation effect can be ignored, $(v_e/c \sim 0)$, the above expression is simplified as follows:

$$\frac{\partial\sigma_i}{\partial\Omega\partial E} \propto \mathrm{Im}\left[\frac{1}{\hat{\varepsilon}}\right]\frac{1}{\theta^2+{\theta_E}^2}. \quad (2)$$

The left side of Figure 2 was calculated by ignoring the retardation effect, while the right side included the influence of the retardation effect. The white frame in Figure 2 shows the notable difference in the retardation calculation. In other words, the retardation effect still seemed to influence the measurements at scattering angles less than 0.2 mrad in the energy loss range of 10–15 eV, even though we used a low accelerating voltage of 60 kV.

To more clearly reveal the influence of the retardation effect, we calculated the SSD by integrating the loss probability to each collection semi-angle, as shown in Figure 3. At a collection semi-angle of 2 mrad, influence of the retardation was not clear. Conversely, the SSD intensity—calculated by assuming a smaller collection semi-angle (0.3 mrad)—increased in the energy range of 10–20 eV due to the retardation effect. Figure 4 shows the dielectric function obtained by the calculated SSD assuming the retardation effect. The collection semi-angle was set to 0.3 mrad. The experimentally obtained dielectric function was plotted in the figure, too. The calculated dielectric function did not agree in the optical data; in addition, it duplicated the feature of the experimentally obtained dielectric function. It is concluded that the TEM-EELS cannot provide the

correct dielectric function when the influence of the retardation is relatively strong.

In the present situation, using the conventional KKA procedure is problematic because it uses the following equation for the angular correction based on Eq. (2):

$$\mathrm{SSD}(E) = A \cdot \mathrm{Im}\left[\frac{1}{\hat{\varepsilon}}\right] \ln\left(1 + \frac{\beta^2}{{\theta_E}^2}\right), \tag{3}$$

where A is a constant that depends on the electron beam intensity and sample thickness, and β is the correction semi-angle. However, when the influence of the retardation effect is relatively strong, it is necessary to modify Eq. 3 as follows:

$$\mathrm{SSD}(E) = A \cdot \mathrm{Im}\left[\frac{1}{\hat{\varepsilon}} \cdot \{1 - \hat{\varepsilon}(v_e/c)^2\} \cdot \ln\left\{1 + \frac{\beta^2}{{\theta_E}^2(1-\hat{\varepsilon}(v_e/c)^2)}\right\}\right] \tag{4.a}$$

$$= A \cdot \mathrm{Im}\left[\frac{1}{\hat{\varepsilon}} \cdot \{B(\varepsilon) + iC(\varepsilon)\}\right] \tag{4.b}$$

where

$$B(\hat{\varepsilon}) + iC(\hat{\varepsilon}) = \{1 - \hat{\varepsilon}(v_e/c)^2\} \cdot \ln\left\{1 + \frac{\beta^2}{{\theta_E}^2(1-\hat{\varepsilon}(v_e/c)^2)}\right\}. \tag{5}$$

From Eq. 4, the ELF ($\mathrm{Im}[1/\hat{\varepsilon}]$) clearly cannot be directly extracted from the SSD. Here we rewrite the Eq. 4 as:

$$A \cdot \mathrm{Im}\left[\frac{1}{\hat{\varepsilon}}\right] = \left\{\mathrm{SSD}(E) - A \cdot \mathrm{Re}\left[\frac{1}{\hat{\varepsilon}}\right] C(\hat{\varepsilon})\right\} / B(\hat{\varepsilon}). \tag{6}$$

In this study, we extracted the loss function from the measured SSD

according to the following procedure.

a) Set a predicted dielectric function $\varepsilon^p = \varepsilon_1^p + i\varepsilon_2^p$.

b) Put ε^p into the right-hand side of the Eq. 6 and estimate the ELF.

c) After normalizing the ELF, calculate a corrected dielectric function (ε^c) by using the KKA.

d) Remove the surface loss contribution from the SSD in the same way as in the conventional KKA procedure.

e) Repeat the above routine a)~d) until the dielectric function becomes self-consistent ($\varepsilon^c = \varepsilon^p$).

Figure 5 shows a flowchart summary of this procedure. Usually we set to the initial value of the predicted dielectric function as $\varepsilon^p = 0$, and redefined the ε^p value by ${\varepsilon^p}_{new} = x \cdot \varepsilon^c + (1-x){\varepsilon^p}_{old}$ during the iterations, where x is the mixing parameter ($0 < x \leq 1$).

Using the improved KKA procedure, as described above, we give the corrected dielectric functions in Figure 6. Practically, when the mixing parameter of x = 0.04 was used in every iteration step, we reached within 1% error between the $\varepsilon^c(0)$ and $\varepsilon^p(0)$ after the 100 iterations. In addition, we constrained that the values of $\varepsilon_1^p(E) \cdot (v_e/c)^2$ did not exceed 1. Compared

with the results in Figure 1, the corrected dielectric functions agree fairly well with the optical data in the energy range of 10–15 eV. Of note, the plateau of the real part of the dielectric function appears around 10 eV for the larger collection-semi angle (2 mrad), though the influence of the retardation would be effectively small. In other words, we demonstrated that using TEM-EELS and the improved KKA procedure can produce a more accurate dielectric function.

It is generally believed that the momentum dependence of the dielectric function in α-Al_2O_3 is small because its valence electron band is quite flat [14]. In this situation, the influence of the retardation effect is reduced by acquiring the VEEL spectra with a larger collection semi-angle to dampen the retardation effect. However, when measuring the dielectric function of materials with a curved band structure (e.g., Si), the spectra must be acquired with a collection semi-angle as small as possible to avoid the influence of momentum transfer [8]. For such materials, our present technique might be advantageous in measuring VEELS data for KKA.

Finally, we discuss the limitation of the present technique for the VEELS analysis. We applied this technique in the condition that Cerenkov

radiation produced but failed to deduce the correct dielectric function. Figure 7 shows low-loss spectra and SSD of α-Al_2O_3 acquired by TEM operated at 60 kV and 300 kV with the collection semi-angle of 2 mrad. In the case of 300 kV TEM, an obvious loss intensity due to Cerenkov radiation was seen below the bandgap energy of 9 eV (indicated by arrows in the figure). Comparisons of calculated and experimentally obtained SSD were shown in Figure 8(a) and (b). At the accelerating voltage of 60 kV, the calculated SSD considering the retardation effect showed a good agreement with the experimental data. On the other hand, the SSD calculated based on the Eq. 1 never reproduced the loss intensity at the energy less than 9 eV when the accelerating voltage was assumed to 300 kV. This implies that the Eq. 1 cannot provide the correct Cerenkov loss intensity at the energy range in which the imaginary part of the dielectric function equals zero. Figure 9 shows the dielectric functions obtained by conventional and improved KKA procedure; both the dielectric functions acquired by 300 kV TEM could not reproduce the optical data. Particularly, the shape of dielectric function was hardly corrected in the energy region lower than bandgap even if we used the improved KKA procedure. Unfortunately the present technique cannot apply under the

occurrence of Cerenkov radiation due to the imperfection of the equation of Cerenkov loss probability. Another limitation is caused by the influence of surface loss. It is well known that the intensity of Cerenkov radiation effectively reduced by decreasing the sample thickness [4-6]. In normal KKA procedure, the surface loss intensity is effectively removed by assuming the energy loss caused by single surface. However, it was reported that the surface loss based on the light guiding mode became stronger in thinner samples and altered the shape of low-loss spectrum [6], whereas the influence of Cerenkov radiation was effectively suppressed by decreasing the sample thickness. Therefore, both the conventional and improved KKA procedures may not be accurate for thinner specimens. Further improvement of the KKA routine is needed to remove the contributions of the surface loss caused by the light guiding mode and Cerenkov radiation from the experimentally obtained VEEL spectra.

Concluding remarks

We improved the KKA routine for measuring the dielectric function of α-Al_2O_3 to avoid the retardation effect in TEM-EELS. Obvious differences

between the VEELS and optical data appeared in the energy range of 10–20 eV due to the retardation effect, even though the electrons in the medium were traveling slower than the speed of the light. Using the improved KKA procedure and VEELS measurements, we reproduced dielectric functions that agreed with the optical data. Our technique is particularly useful for measuring a dielectric function with a small collection semi-angle.

Acknowledgments

We gratefully acknowledge Mr. K. Ohkubo, Mr. R. Oota, Mr. T. Tanioka, and Ms. Yamanouchi for their technical support in TEM operation. Part of this work was conducted at Hokkaido University, supported by the "Nanotechnology Platform" Program of the Ministry of Education, Culture, Sports, Science and Technology (MEXT), Japan.

References

1. Kohno H, Mabuchi T, Takeda S, Kohyama M, Terauchi M, Tanaka M (1998) Dielectric properties of extended defects in silicon studied by high-resolution transmission EELS, *J. Electron Microsc.* 47: 311–317.

2. Brockta G, Lakner H (2000) Nanoscale EELS analysis of dielectric function and bandgap properties in GaN and related materials, *Micron* 31: 435–440.

3. Sato Y, Terauchi M, Saito Y, Sato K, Saito R (2008) Relation between peak structures of loss functions of single double-walled carbon nanotubes and interband transition energies, *J. Electron Microsc.* 57: 129–132.

4. Stöger-Pollach M, Franco H, Schattschneider P, Lazar S, Schaffer B, Grogger W, Zandbergen H W (2006) Čerenkov losses: A limit for bandgap determination and Kramers–Kronig analysis, *Micron* 37: 396–402.

5. Stöger-Pollach M, Schattschneider P (2007) The influence of relativistic energy losses on bandgap determination using valence EELS, *Ultramicroscopy* 107:1178–1185.

6. Erni R, Browning N D (2008) The impact of surface and retardation losses on valence electron energy-loss spectroscopy, *Ultramicroscopy* 108: 84–99.

7. Potapov P L, Engelmann H-J, Zschech E, Stöger-Pollach M (2009) Measuring the dielectric constant of materials from valence EELS, *Micron* 40: 262–268.

8. Stöger-Pollach M (2008) Optical properties and bandgaps from low loss

EELS: Pitfalls and solutions, *Micron* 39: 1092–1110.

9. Horák M, Stöger-Pollach M (2015) The Čerenkov limit of Si, GaAs and GaP in electron energy loss spectrometry, *Ultramicroscopy* 157: 73–78.

10. Erni R (2016) On the validity of the Čerenkov limit as a criterion for precise band gap measurements by VEELS, *Ultramicroscopy* 160: 80–83.

11. Egerton R F (2011) *Electron energy-loss spectroscopy in the electron microscope, 3rd edition.* (Springer, New York.)

12. Arakawa E T, Williams M W (1968) Optical properties of aluminum oxide in the vacuum ultraviolet, *J. Phys. Chem. Solids* 29: 735–744.

13. Kröger E (1970) Transition radiation, Cerenkov radiation and energy losses of relativistic charged particles traversing thin foils at oblique incidence theoretical calculations and numerical computations, *Z. Physik* 235: 403–421.

14. Perevalov P V, Shaposhnikov A V, Gritsenko V A, Wong H, Han J H, Kim C W (2007) Electronic structure of α-Al_2O_3: ab initio simulations and comparison with experiment, *JETP Letters* 85: 165–168.

Figure captions:

Fig. 1 Real (ε_1) and imaginary (ε_2) parts of dielectric functions obtained by VEELS and KKA at various collection semi-angles. The dotted line shows the measured optical data [12].

Fig. 2 Calculated double-differential cross-section of the inelastic scattering in α-Al_2O_3 for 60-keV electrons with (right) and without (left) the retardation effect.

Fig. 3 Calculated SSD with and without the retardation effect. The collection semi-angles were set to (a) 0.3 mrad and (b) 2 mrad.

Fig. 4 Dielectric function obtained by calculated SSD with the retardation effect. The collection semi-angles was set to 0.3 mrad.

Fig. 5 Flowchart showing the present procedure for deriving the dielectric function.

Fig. 6 Corrected dielectric functions obtained by the improved KKA

procedure.

Fig. 7　(a) Low-loss spectra and (b) SSD of α-Al_2O_3 acquired using 60 kV and 300 kV TEM. The bandgap energy was indicated by arrow in the figure.

Fig. 8　SSD obtained by VEELS together with calculated SSD. The accelerating voltages of TEM were (a) 60 kV and (b) 300 kV.

Fig. 9　Dielectric functions calculated by the (a) conventional and (b) improved KKA procedures under the occurrence of Cerenkov radiation.

Fig.1

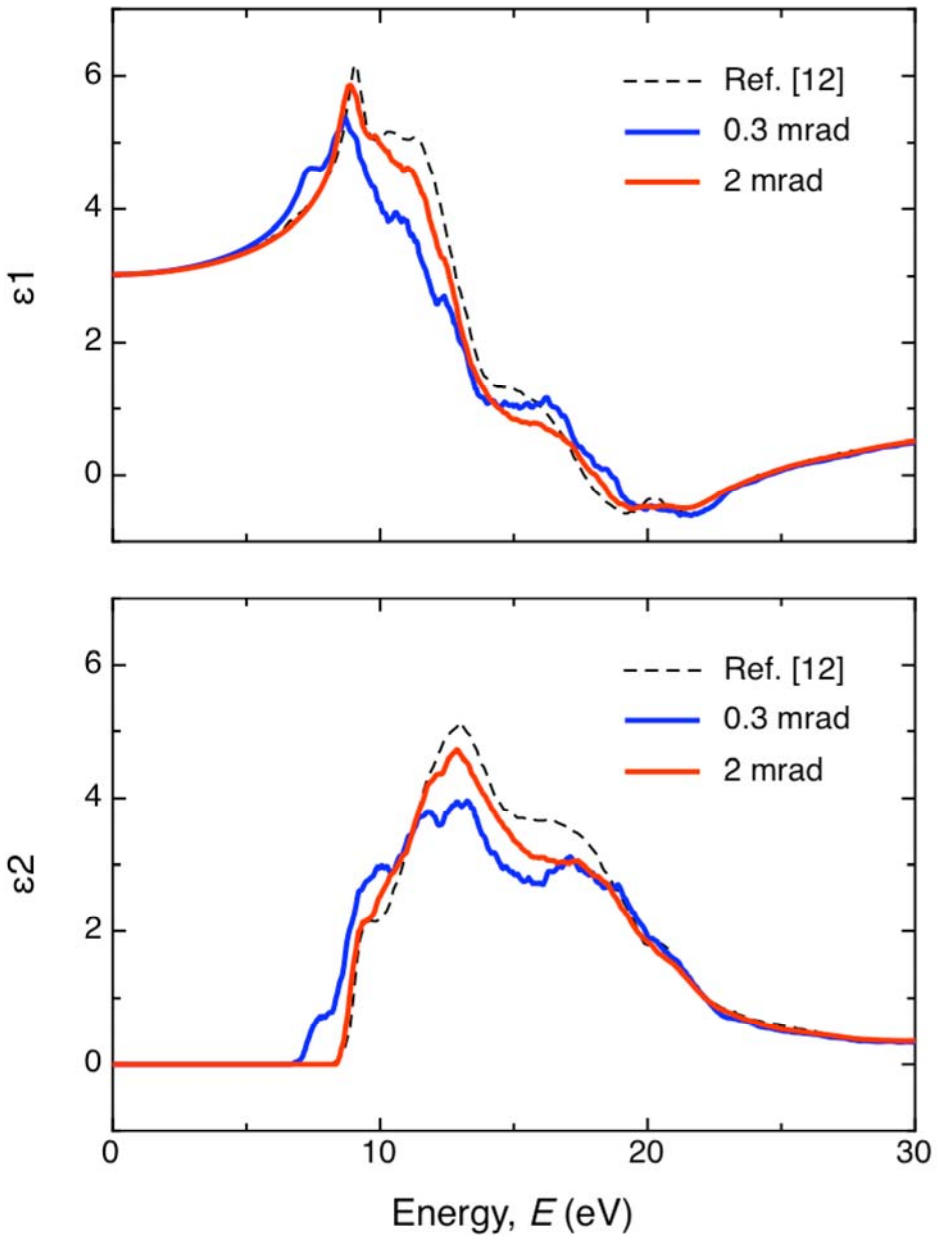

Fig.2

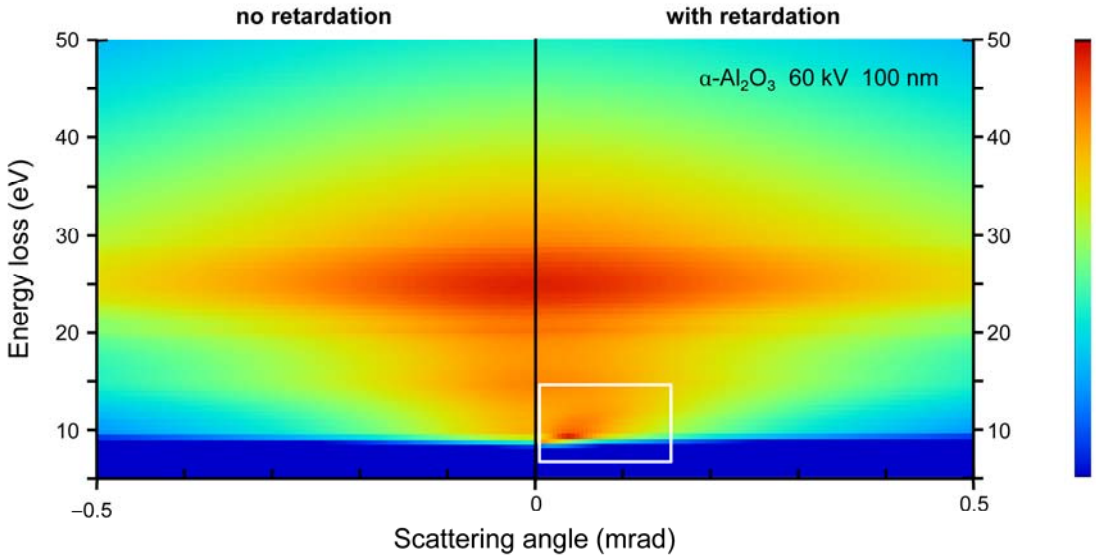
no retardation
with retardation
α-Al2O3 60 kV 100 nm
Energy loss (eV)
50
40
30
20
10
−0.5
0
0.5
Scattering angle (mrad)

Fig.3

(a) 0.3 mrad

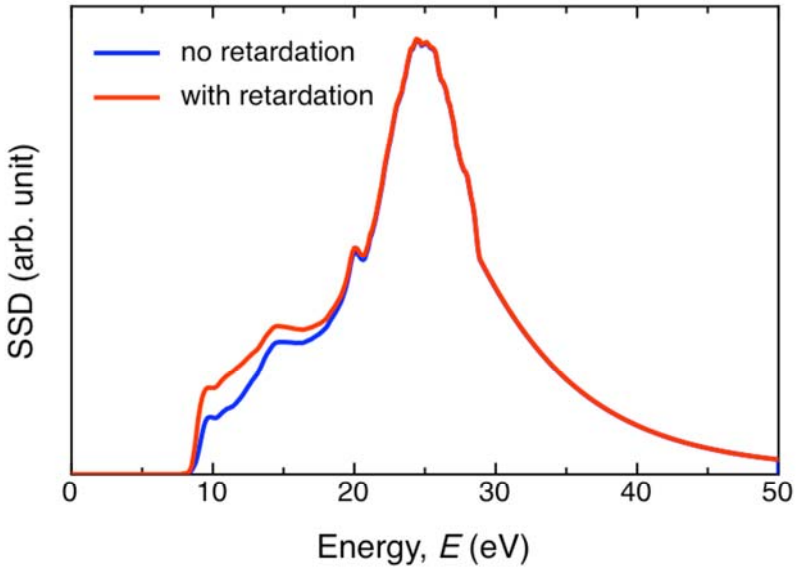

(b) 2 mrad

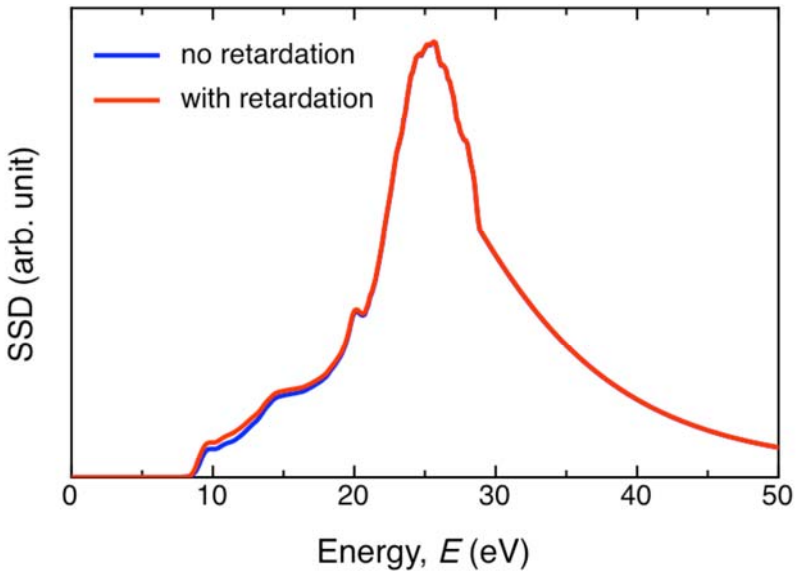

Fig.4

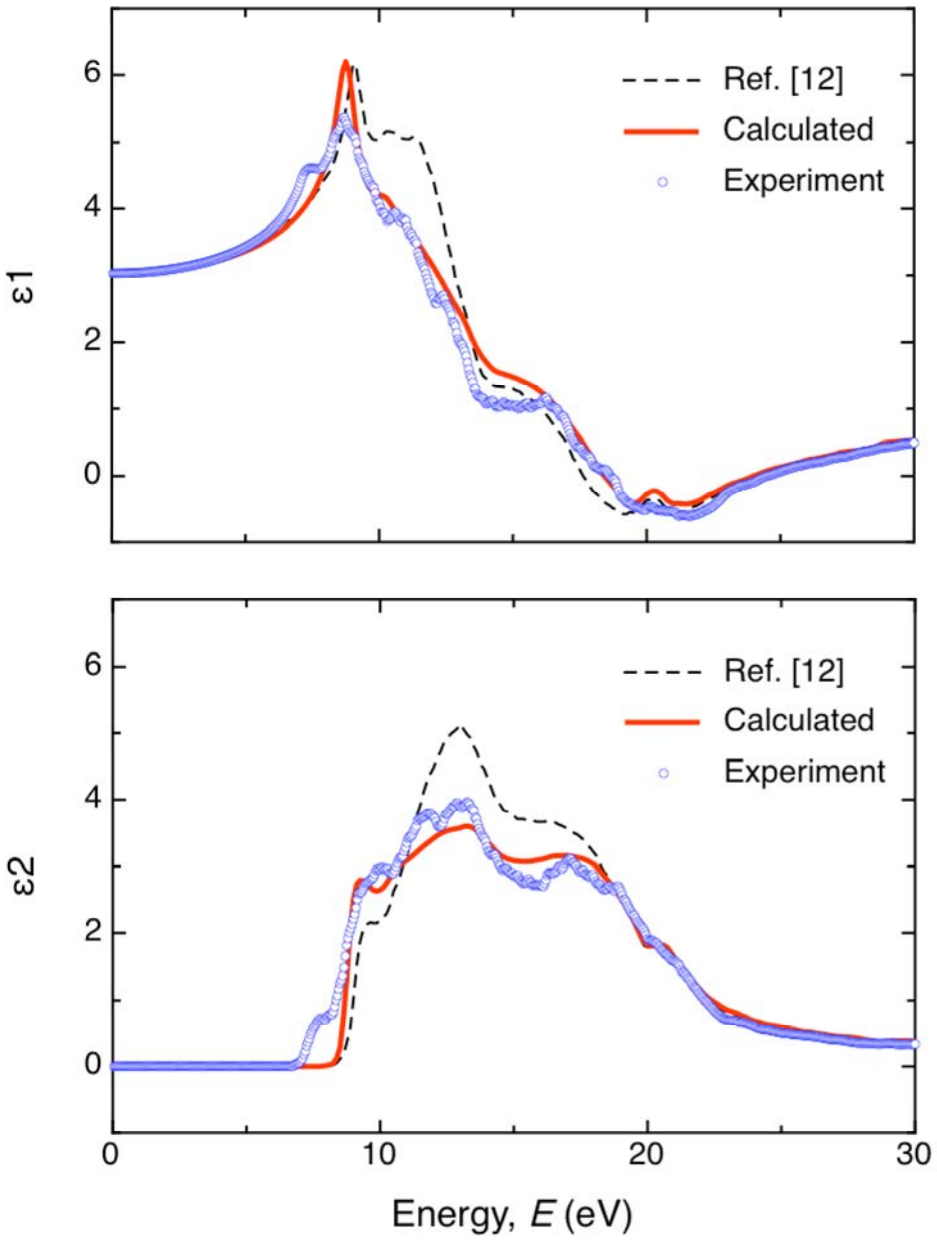

Fig.5

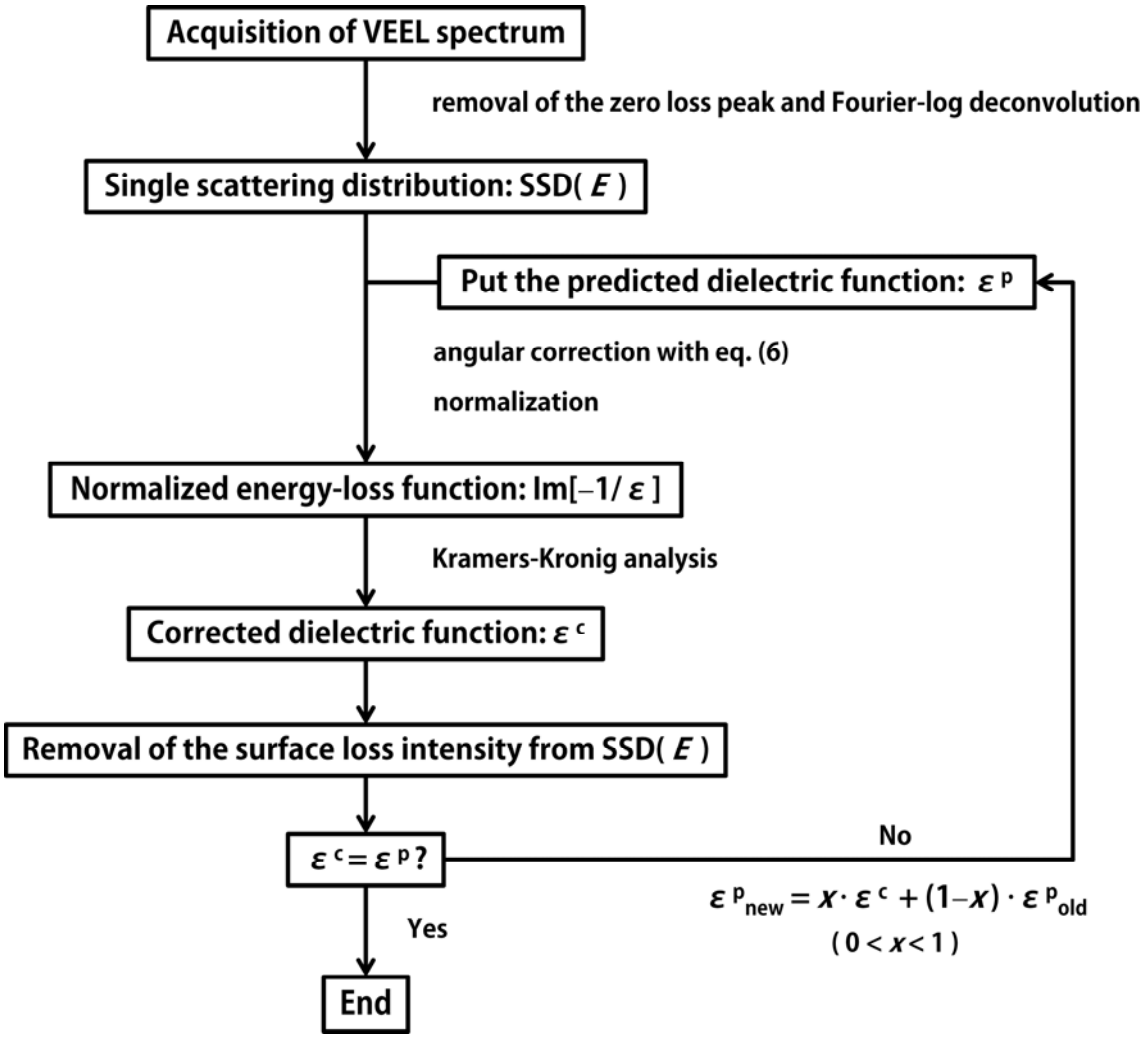
Acquisition of VEEL spectrum
removal of the zero loss peak and Fourier-log deconvolution
Single scattering distribution: SSD(E)
Put the predicted dielectric function: ε p
angular correction with eq. (6)
normalization
Normalized energy-loss function: Im[−1/ ε]
Kramers-Kronig analysis
Corrected dielectric function: ε c
Removal of the surface loss intensity from SSD(E)
ε c = ε p ?
No
ε p new = χ · ε c + (1−χ) · ε p old
(0 < χ < 1)
Yes
End

Fig.6

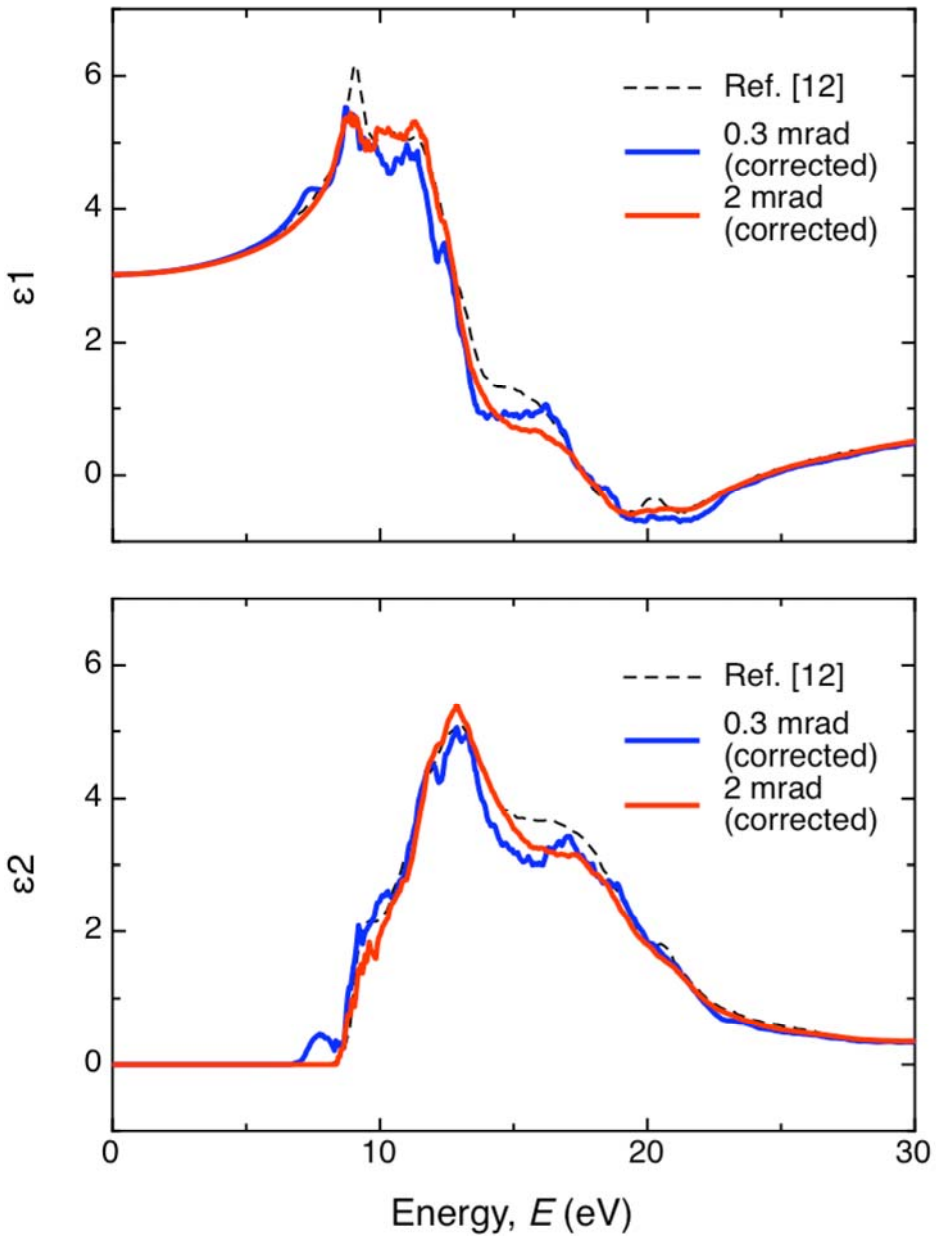
ε1
ε2
Ref. [12]
0.3 mrad (corrected)
2 mrad (corrected)
0
2
4
6
0
10
20
30
Energy, E (eV)

Fig.7

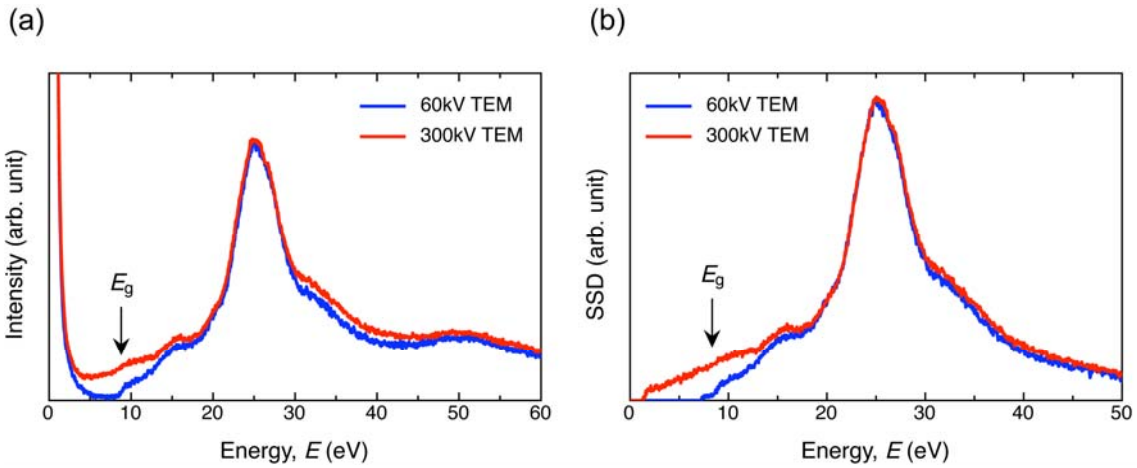
(a)
(b)
60kV TEM
300kV TEM
Intensity (arb. unit)
SSD (arb. unit)
E_g
Energy, E (eV)

Fig.8

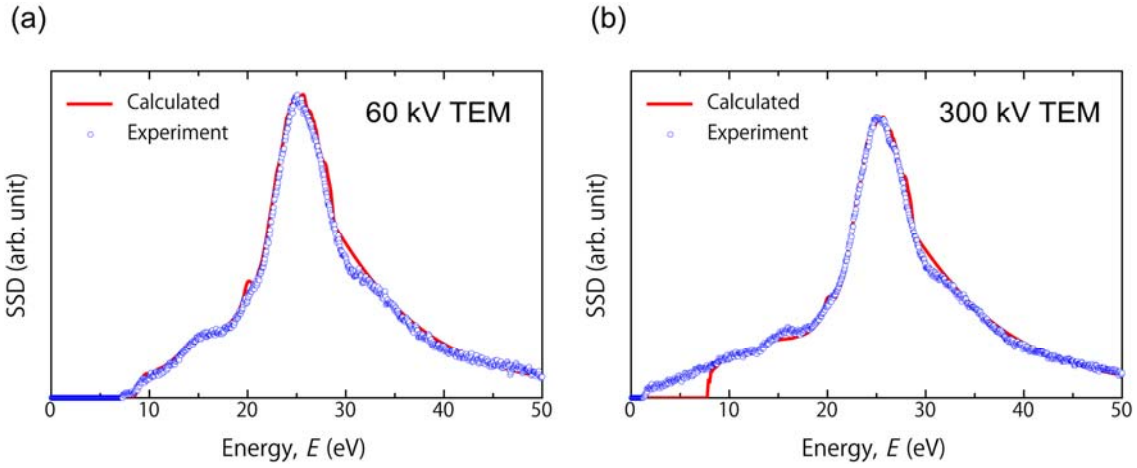
(a)
(b)
Calculated
Experiment
60 kV TEM
300 kV TEM
SSD (arb. unit)
Energy, E (eV)

Fig.9

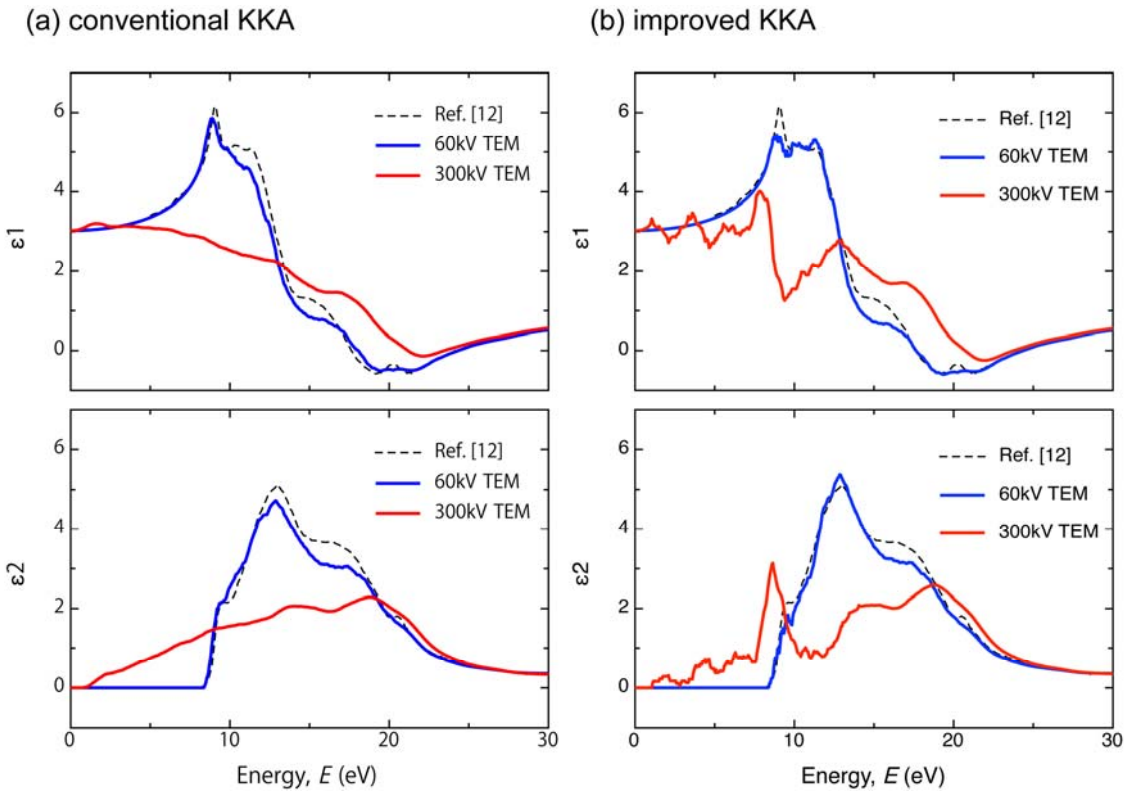
(a) conventional KKA
(b) improved KKA
ε1
ε2
Ref. [12]
60kV TEM
300kV TEM
Energy, E (eV)
0
2
4
6
10
20
30